

Stellar Wind Erosion of Protoplanetary Discs

N. R. Schnepf^{1*}, R. V. E. Lovelace², and M.M. Romanova²

¹Earth, Atmospheric and Planetary Sciences,

Massachusetts Institute of Technology, Cambridge, 02139 MA, USA

²Department of Astronomy, Cornell University, Ithaca, 14853 NY, USA

December 3, 2024

Abstract

An analytic model is developed for the erosion of protoplanetary gas discs by high velocity magnetized stellar winds. The winds are centrifugally driven from the surface of rapidly rotating, strongly magnetized young stars. The presence of the magnetic field in the wind leads to Reynolds numbers sufficiently large to cause a strongly turbulent wind/disk boundary layer which entrains and carries away the disc gas. The model uses the conservation of mass and momentum in the turbulent boundary layer. The time-scale for significant erosion depends on the disc accretion speed, accretion rate and on the wind mass loss rate. The time-scale is estimated to be $\sim 2 \times 10^6$ yr. The stellar wind erosion may act in conjunction with photo-evaporation of the discs.

Keywords stars: pre-main sequence: stars: T Tauri stars — magnetic fields: general: accretion, accretion disks: protoplanetary discs: stars: winds, outflows

1 Introduction

A wide body of observations establish that the lifetime of gaseous protoplanetary discs is relatively short. While most protostars younger than 10^6 yr have gaseous discs, only 50% of protostars 3×10^6 yr in age have gaseous discs and very few stars 6×10^6 yr or older have a gaseous discs (Armitage 2010). Spectroscopic observations of the hot continuum radiation produced when infalling gas impacts the stellar surface, it is known that the accretion rate of gas onto a star decays on a similar time-scale (Hartmann et al. 1998). Observations also suggest that the dispersal of gas occurs on a wide range of disc radii during a short time-scale (Skrutskie et al. 1990; Wolk & Walter 1996; Andrews & Williams 2005).

The short lifetime of a gaseous disc plays a critical role in the formation of planetary systems. It directly affects the time available for

*E-mail: nschnepf@mit.edu

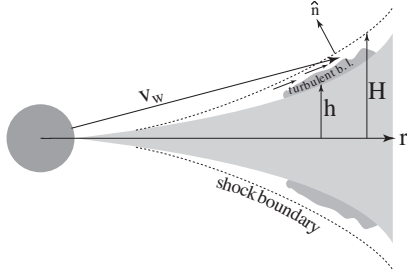


Figure 1: A cross-section of the protoplanetary disc with the disc-wind turbulent boundary layer ($h < z < H$) and outer oblique shock shown. \hat{n} is the normal to the shock wave, \mathbf{v}_w is the wind velocity, h is the disc half-thickness and H is the vertical height of the shock.

planetesimals to agglomerate additional material, as well as the migration of planets within the disc (Armitage 2010; Zsom et al. 2010). The mechanisms by which the gas is lost may play an important role in the formation of planetary systems.

A class of protoplanetary discs termed *transition discs* have been identified by a dip in the mid-infrared spectra which can be modeled by a reduced surface density of dust in the inner regions ($\lesssim 35$ au) of the discs (Espaillat et al. 2007). Sub-millimeter imaging directly shows a deficit in surface density of dust in these systems (e.g., Piétu et al. 2007). The observations suggest an inside-out dispersal of the dust possibly caused by photo-evaporation (Clarke et al. 2001; Owen et al. 2012), by the presence of giant planets, or by other processes (Birnstiel et al. 2013). Photo-evaporative destruction of discs is thought to occur when the photo-evaporative mass-loss rate \dot{M}_{pe} exceeds the accretion rate \dot{M}_d onto the star (e.g., Richling & Yorke 1997; Hollenbach et al. 2000). Additionally, the dust's radial distribution is influenced by grain growth, migration, destruction via collisions, and trapping in vortices excited at the outer gap edge caused by giant planets (Regály et al. 2012). The transition discs have lower accretion rates than younger standard discs, but not sufficiently low for photo-evaporation to explain the large sizes of the regions of low dust density (Birnstiel 2013).

It appears likely that multiple processes including photo-evaporation are involved in the dissipation of the dust and gas in protoplanetary discs. This work analyzes the erosion of the gas component of discs caused by high-velocity magnetized stellar winds where the presence of the magnetic field leads to Reynolds numbers sufficiently large to cause a strongly turbulent wind and disk boundary layer (see Figure 1) as suggested by Lovelace et al. 2008. Initially, the disc mass is constituted predominantly of gas. Strongly magnetized winds from young stars with discs are likely because the stars are known to rotate rapidly and to be strongly magnetized. Wind erosion of protostellar stellar disc has been discussed in a number of previous works as reviewed by Hollenbach et al. (2000).

However, the important role played by a rapidly rotating star’s magnetic field in launching a high velocity wind has apparently not been considered. Furthermore, the role of the wind’s magnetic field in producing a strongly turbulent wind and disc boundary layer has not been discussed.

Section 2 of the paper discusses magnetized stellar winds. Section 3 gives estimates of the gas erosion rates due to the winds, and Section 4 gives a specific model calculation of the evolution of the disc’s gas surface density $\Sigma_d(r, t)$. Section 5 gives the conclusions of this work.

2 Magnetized Stellar Winds

The winds from rotating magnetized stars may be thermally driven as in the Solar wind. The magnetic field has an important role in the outward transport of angular momentum by the wind (Weber & Davis 1967; Matt & Pudritz 2008a,b). For thermally driven winds from slowly rotating stars, the radial flow velocity at large distances is the Parker velocity $v_P = [2c_{s0}^2/(\gamma - 1) - 2GM_*/R_*]^{1/2}$, where c_{s0} is the sound speed at the star’s radius R_* , M_* is the star’s mass, and γ is the specific heat ratio. [Note that both spherical (R, θ, ϕ) and cylindrical (r, ϕ, z) inertial coordinates are used in this work.]

In contrast, for conditions where the thermal speed of the gas close to the star is small (compared with the escape velocity), where the star’s magnetic field is strong, and where the star rotates rapidly, there are magnetically driven winds (also termed fast magnetic rotator, FMR, winds) (Michel 1969; Belcher & MacGregor 1976). These winds are driven by the centrifugal force of the star’s rapidly rotating magnetic field rather than the thermal energy in the star’s corona. For a rotating magnetized star, the radial wind velocity at large distances from the star is $v_w = 1.5[\Omega_*^2(B_{R_*}R_*^2)/\dot{M}_w]^{1/3}$ (Michel (1969), where $P_* = 2\pi/\Omega_*$ is the rotation period of the star and $B_{R_*} = B_R(R_*)$. The characteristic acceleration distance of the winds is the Alfvén radius of the wind, $R_{Aw} = (2/3)^{1/2}(v_w/\Omega_*)$ (Belcher & MacGregor 1976). For a star with rotation period $P_* = 10$ d, a radius twice the radius of the Sun, $R_* = 1.4 \times 10^{11}$ cm (Armitage & Clarke 1996), a surface magnetic field $B_{R_*} = 0.5$ kG, and $\dot{M}_w = 10^{-10}M_\odot/\text{yr}$, one finds $v_w \approx 1400$ km/s, and $R_{Aw} \approx 1$ au. For the magnetic acceleration of the solar wind to be important, the product of the rotation rate Ω_* times the magnetic flux per steradian $B_{R_*}R_*^2$ would need to be ~ 20 times larger than the present values (Belcher & MacGregor 1976). The magnetic winds cause the rapid spin-down of the stars on a time-scale $T_{sdw} = I[(2/3)R_{Aw}^2\dot{M}_w]^{-1}$, where I is the moment of inertia of the star (Weber & Davis 1967; Belcher & MacGregor 1976). This time-scale may be as short as $\sim 10^6$ yr. However, the spin-down torque of the wind is strongly dominated by the spin-up torque due to the disc accretion to the star for accretion rates $\sim 10^{-8}M_\odot/\text{yr}$. This spin-up torque acts to balance the spin-down torque due to the magnetic coupling of the star’s magnetic field to the inner region of the disc (see Long et al. 2005; Matt & Pudritz 2008a,b).

The magnetic fields of classical T Tauri stars (CTTSs) are typically in the kG range (Johns-Krull & Valenti 2000; Johns-Krull 2007)). Fur-

thermore, these stars typically rotate rapidly with periods $\sim 2 - 15$ d (Bouvier et al. 1993). Thus magnetically driven winds may be important for T Tauri stars.

Magnetically driven stellar winds have been found in magnetohydrodynamic (MHD) simulations of rapidly-rotating, disk-accreting stars particularly in the “propeller” regime (Romanova et al. 2005; Ustyugova et al. 2006; Lovelace et al. 1999). The winds are found to flow in opposite directions along the rotation axis transporting energy and angular momentum away from the star. For the case of an aligned dipole field, the field acts to block an equatorial outflow. However, for multipolar fields, winds are expected in all directions from the star’s surface.

In deriving the evolution of disc density due to this magnetized wind, it is useful to consider the physical conditions in the wind at a distance of $R = 1$ au from the sun with fiducial conditions of wind density $n_w = 10^5$ cm^{-3} , wind speed $v_w = 10^3$ km/s, a predominantly toroidal time averaged magnetic field $B_w = 0.1$ G, and ion (proton) and electron temperatures of $T_i = T_e = 10^5$ K. From this distance and beyond, (i) the wind velocity is predominantly radial, (ii) it is super fast magnetosonic, and (iii) it is much larger than the Keplerian velocity of the disc matter.

Under these conditions, the ion and electron gyro-frequencies are $\omega_{ci} \approx 960/\text{s}$ and $\omega_{ce} \approx 1.8 \times 10^6/\text{s}$. The corresponding ion and electron gyro-radii are $r_{gi} \approx 3 \times 10^3$ cm and $r_{ge} \approx 70$ cm. From this, the ion and electron collision times ($\propto T^{3/2}/n$) are $\tau_i \approx 470$ s and $\tau_e \approx 11$ s. The ion and electron mean-free paths are $\ell_i = \ell_e = 1.4 \times 10^9$ cm (Braginskii 1965). Thus, $\omega_{ci}\tau_i \approx 4.6 \times 10^5$ and $\omega_{ce}\tau_e \approx 2 \times 10^7$.

In the absence of a magnetic field, the kinematic viscosities of ions and electrons are $\nu_{0i} \approx v_{th,i}^2\tau_i \approx 4 \times 10^{15}$ cm^2/s and $\nu_{0e} \approx v_{th,e}^2\tau_e \approx 1.7 \times 10^{17}$ cm^2/s , where $v_{th,i,e}$ is the ion or electron thermal speed. Thus, without a magnetic field the Reynolds number, $\text{Re} = rv_w/\nu_{0e} \approx 8800$, is such that boundary layer flow is laminar.

When the magnetic field is included, there are five different viscosity coefficients. Fortunately, for the considered problem the important viscosity coefficient is that for momentum transport across the magnetic field. For example, the momentum flux-density component is $T_{R\theta} = -\rho\nu_{\perp}R^{-1}\partial v_R/\partial\theta$. For ions, the viscosity term is $\nu_{\perp i} \approx \nu_{0i}/(\omega_{ci}\tau_i)^2 \approx 1.9 \times 10^4$ cm^2/s , and for electrons it is $\nu_{\perp e} \approx \nu_{0e}/(\omega_{ce}\tau_e)^2 \approx 440$ cm^2/s . Using the viscosity $\nu_{\perp i}$, the effective Reynolds number for the wind is $\text{Re}_w = Rv_w/\nu_{\perp i} \sim 10^{18}$. Evidently, unlike the non-magnetic case with laminar boundary layer flow, with a magnetic field the boundary layer flow is strongly turbulent. The large reduction of the viscosity results from the particle step size between collisions being a gyro-radius rather than a mean-free path. Thus, the estimated Reynolds number also holds for a turbulent magnetic field.

The relevant heat conductivity coefficient is that for the heat flux across the magnetic field, $q_{\theta} = -\kappa_{\perp}R^{-1}\partial(k_B T)/\partial\theta$, where $\kappa_{\perp} \approx \kappa_{\perp i} \approx 2nv_{th,i}^2\tau_i/(\omega_{ci}\tau_i)^2 \approx 3.8 \times 10^9$ $(\text{cm s})^{-1}$ and where k_B is Boltzman’s constant. For this heat conductivity, the heat flow from the wind into the disc is negligible compared with the energy flux per unit area from the disc [$3GM_*\dot{M}_d/(8\pi R^3)$] for accretion rates $\dot{M}_d \sim 10^{-8}M_{\odot}/\text{yr}$, which is in turn small compared to the irradiation of the disc by the star.

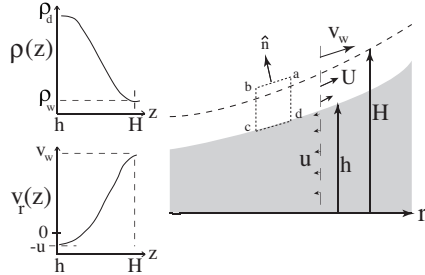


Figure 2: Sketches of the vertical profiles of density ρ and radial velocity $\langle v_r \rangle$ within the boundary layer is shown on the left. Here, ρ_d is the density at the surface of the disc, ρ_w is the density of the wind, and v_w is the speed of the wind.

A weak oblique shock arises where the wind encounters the much denser disc. This occurs at a height $H(r) \ll r$ above the equatorial plane for a disc with half-thickness $h(r) < H(r)$ (Fig. 1). The angle between the incident flow and the shock is $\beta \approx rd(H/r)/dr \ll 1$, with β expected to be > 0 .

After passing through the shock, the flow is deflected by an angle $\delta = 2\beta/(1 + \gamma) = 3\beta/4$ (where $\gamma = 5/3$) away from the equatorial plane and the flow speed is reduced by a small fractional amount. This region between h and H is the boundary layer (shown in Figure 1). The influx of wind matter into this layer is $-d\mathbf{S} \cdot (\rho_w \mathbf{v}_w) \approx dS \rho_w v_w r [d(H/r)/dr]$, where $dS = r dr d\phi$ is the area element of the shock on the top side of the disc. The Keplerian velocity ($v_K = \sqrt{GM/r}$) of the disc is small compared to the wind velocity for $r \geq 1$ au, so it is neglected. The density in the boundary layer varies from $\rho(r, h) \gg \rho_w$ at the surface of the disc to ρ_w at $z = H$. The time-averaged radial flow velocity varies from $|v_r(r, h)| \ll v_w$ to $v_r = v_w$ at $z = H$; $v_r(r, h)$ is neglected.

3 Stationary Conditions

For estimations of the mass loss rate from the disc, it is useful to first consider the loss rate at one instant of time. In Section 4 we treat the time evolution of the disc. For stationary conditions, the conservation of mass and radial momentum in the annular region $a - b - c - d$ (shown in Fig. 2) of the boundary layer on the top side of the disc provides

$$\frac{\partial (r F_r^m)}{\partial r} = r \left[r \frac{d(H/r)}{dr} \right] \rho_w v_w + \frac{1}{4\pi} \frac{d\dot{M}_d}{dr}, \quad (1)$$

$$\frac{\partial (r F_r^p)}{\partial r} = r \left[r \frac{d(H/r)}{dr} \right] \rho_w v_w^2. \quad (2)$$

The terms on the left-hand sides are due to the vertical sides of the region and the right-hand side is due to the sides $a - b$ and $c - d$. Here, F_r^m is the

mass flux and F_r^p is the radial momentum flux both per unit circumference of the top side of the disc,

$$F_r^m = \int_h^H dz \langle \rho v_r \rangle, \quad F_r^p = \int_h^H dz \langle \rho v_r^2 \rangle. \quad (3)$$

The angular brackets indicate averages are over the turbulent fluctuations. The mass-loss rate of the disc per unit radius due to entrainment is $d\dot{M}_d/dr$. The disc matter influx to the boundary layer brings in negligible radial momentum.

We can integrate equations (1) and (2) from the inner radius of the disc r_{in} , where F_r^m and F_r^p are negligible, to an arbitrary radius in disk the radius r . The average radial velocity in the boundary layer is

$$U(r) = \frac{F_r^p(r)}{F_r^m(r)}. \quad (4)$$

We can obtain an equation for the mass loss rate due to erosion from the top and bottom sides of the disk between $r = r_{\text{in}}$ and r ,

$$\dot{M}_{\text{der}} = 4\pi \left(\frac{v_w}{U} - 1 \right) \int_{r_{\text{in}}}^R r dr \left[r \frac{d(H/r)}{dr} \right] \rho_w v_w. \quad (5)$$

We assume a spherically symmetric wind with constant mass outflow rate $\dot{M}_w = \text{const}$ and a constant wind speed $v_w = \text{const}$, so that $\rho_w v_w = \dot{M}_w / (4\pi r^2)$. This allows evaluation of the mass loss rate of the disc,

$$\dot{M}_{\text{der}} = \left(\frac{v_w}{U} - 1 \right)_{\text{out}} \left(\frac{H}{r} \right)_{\text{out}} \dot{M}_w. \quad (6)$$

The main unknown function in this equation is $U(r)$.

The average velocity U depends on the vertical profiles of density and radial velocity which are not known. We expect the profiles, for example $\langle v_r(z) \rangle$, to be substantially different from those of laboratory turbulent boundary layers over solid surfaces where $\rho = \text{const}$ (e.g., Schlichting 1968; Roy & Blottner 2006). The main reason for the difference is that the density at the surface of the disc $\rho(r, h)$ is many orders of magnitude larger than the wind density ρ_w . For a laboratory boundary layer, a mixing-length model of the momentum transport gives $(z')^2 (d\langle v_r \rangle / dz')^2 = \text{const}$, where $z' \equiv z - h$, and this gives the well-known logarithmic velocity profile (see e.g. Schlichting 1968). For this profile most of the change of velocity is quite close to the wall ($z' = 0$). In contrast, for the disc boundary layer a mixing length model gives $\rho(z') (z')^2 (d\langle v_r \rangle / dz')^2 = \text{const}$. Because of the density dependence, the change in the velocity occurs relatively far from the wall. An important consequence of this is that the average velocity U is much smaller than v_w , because U is the density weighted average radial velocity. If we make the weak assumption that U is less than $v_w/2$, then we have a lower limit on the disc mass loss rate $\dot{M}_d \gtrsim (H/r)_{\text{out}} \dot{M}_w$. For an initial disc mass of $M_d = 0.02 M_\odot$ (e.g., Kuchner 2004), $(H/r)_{\text{out}} = 0.3$, and $\dot{M}_w = 10^{-10} M_\odot/\text{yr}$, the disc loss time is $T_d \lesssim M_d / \dot{M}_{\text{der}} = 6.7 \times 10^8$ yr. This is much longer than the average disc lifetime.

However, the above discussion suggests that U is much less than v_w . On the other hand U is necessarily larger than the local escape velocity $v_{\text{esc}} = (2GM_*/r)^{1/2}$ in order for the matter flow in the boundary layer to become unbound from the star. Here, M_* is the mass of the star. Thus we find an upper bound on the mass loss rate from the disc due to the wind

$$\begin{aligned} \dot{M}_{\text{der}} &\lesssim \left(\frac{v_w H}{v_{\text{esc}} r} \right)_{\text{out}} \dot{M}_w, \\ &\lesssim 240 \left(\frac{v_w}{10^3 \text{ km/s}} \right) \left(\frac{r_{\text{out}}}{10^2 \text{ au}} \right)^{1/2} \left(\frac{(H/R)_{\text{out}}}{0.3} \right) \dot{M}_w, \end{aligned} \quad (7)$$

assuming $v_{\text{esc}} \ll v_w$. For an initial disc mass of $M_d = 0.02 M_\odot$, $(H/r)_{\text{out}} = 0.3$, $r_{\text{out}} = 10^2$ au, and $\dot{M}_w = 10^{-10} M_\odot/\text{yr}$, the disc loss time is $T_d \gtrsim M_d/\dot{M}_{\text{der}} \approx 0.8 \times 10^6$ yr. This is shorter than the average disc lifetime.

4 Non-Stationary Evolution

In the absence of wind erosion conservation of the disc matter gives

$$\frac{\partial(2\pi r \Sigma_d)}{\partial t} - \frac{\partial(2\pi r u \Sigma_d)}{\partial r} = 0, \quad (8)$$

where

$$\Sigma_d(r, t) = \int_{-h}^h dz \rho(r, z, t), \quad u(r, t) = -\frac{1}{\Sigma_d} \int_{-h}^h dz \rho v_r, \quad (9)$$

with $u \geq 0$ being the accretion speed of the disc matter.

For stationary conditions, $ru\Sigma_s = \text{const}$. We assume an α -disc model (Shakura & Sunyaev 1973), $u = \alpha c_s^2/v_K$, where $\alpha = \text{const} \sim 10^{-3} - 0.1$, c_s is the midplane isothermal sound speed, and v_K is the Keplerian velocity of the disc. Commonly considered models have $\Sigma_d \propto r^{-q}$ with $q = \text{const} \sim 1$. This implies that $T \propto r^{q-3/2}$ and $u \propto r^{q-1}$. The disc is assumed to be in hydrostatic equilibrium in the vertical direction so that $h/r = c_s/v_K$ and thus $h/r \propto r^{q/2-1/4}$. For specificity we adopt $q = 1$ so that $u = \text{const}$ and $h/r \propto r^{1/4}$.

With the wind erosion included we assume that u and h/r are the same as in a stationary disc in the region where $\Sigma_d(r, t) > 0$. Further, we assume that the surface density in the top and bottom boundary layers, $\Sigma_{\text{bl}} = 2 \int_h^H dz \rho$, is much smaller than Σ_d . Mass conservation then gives

$$\begin{aligned} \frac{\partial(2\pi r \Sigma_d)}{\partial t} - \frac{\partial(2\pi r u \Sigma_d)}{\partial r} \\ = -4\pi \frac{\partial(r F_r^m)}{\partial r} + 4\pi r^2 \left[\frac{d}{dr} \left(\frac{H}{r} \right) \right] \rho_w v_w \end{aligned} \quad (10)$$

where F_r^m is given in Equation 3.

Conservation of momentum in the radial direction gives

$$\frac{\partial(2\pi r \Sigma_{\text{bl}} U)}{\partial t} + \frac{\partial(4\pi r F_r^p)}{\partial r} = 4\pi r^2 \left[\frac{d}{dr} \left(\frac{H}{r} \right) \right] \rho_w v_w^2, \quad (11)$$

where F_r^p is given in Equation and $U(r, t)$ in Equation 4. The term $\partial(2\pi r \Sigma_{\text{bl}} U)/\partial t$ can be neglected because $\Sigma_{\text{bl}} \ll \Sigma_d$. Equation 11 can then be integrated from the inner radius of the disc $r_{\text{in}} i$ where $F_r^m = 0$ to a radius r to give

$$r F_r^m = \frac{\dot{M}_w v_w}{4\pi U} \left[\frac{H}{r} - \left(\frac{H}{r} \right)_i \right], \quad (12)$$

where the i -subscript indicates evaluation at $r = r_{\text{in}}$. We have again assumed for simplicity that the stellar wind is spherically symmetric with both $\dot{M}_w = \text{const}$ and $v_w = \text{const}$ in space and time for $t > 0$. Thus the right-hand side of Equation 10 is

$$\mathcal{R}_{10} = -\dot{M}_w \frac{\partial}{\partial r} \left(\frac{v_w}{U} \left[\frac{H}{r} - \left(\frac{H}{r} \right)_i \right] - \frac{H}{r} \right). \quad (13)$$

Equation 10 can be integrated using the method of characteristics. In view of the fact that $u = \text{const}$, we have

$$\frac{d(2\pi r \Sigma_d)}{dt} = \left(\frac{\partial}{\partial t} - u \frac{\partial}{\partial r} \right) (2\pi \Sigma_d). \quad (14)$$

The characteristics are $r = r_0 - ut$, where r_0 is the radius of the disc fluid element at $t = 0$ with $r_{\text{in}} \leq r_0 \leq r_{\text{out}}$ and r_{out} the outer radius of the disc. At $t = 0$ the surface density of the disc is $\Sigma_{d0} = \Sigma_{0i}(r_{\text{in}}/r)$. Hence

$$\frac{d\hat{\Sigma}_d}{dt} = \frac{\mathcal{R}_{10}}{2\pi r_{\text{in}} \Sigma_{0i}}, \quad (15)$$

where $\hat{\Sigma}_d(r, t) \equiv \Sigma_d(r, t)/\Sigma_{d0}(r)$. Integrating this equation gives

$$\begin{aligned} \hat{\Sigma}_d(r, t) &= 1 + \int_0^t dt \frac{\mathcal{R}_{10}}{2\pi r_{\text{in}} \Sigma_{0i}}, \\ &= 1 + \int_r^{r+ut} dr' \frac{\mathcal{R}_{10}(r')}{2\pi r_{\text{in}} u \Sigma_{0i}}, \\ &= 1 - F(r + ut) + F(r), \end{aligned} \quad (16)$$

where

$$F(r) = \frac{\dot{M}_w}{\dot{M}_{d0}} \left(\frac{v_w}{U(r)} \left[\frac{H}{r} - \left(\frac{H}{r} \right)_i \right] - \frac{H}{r} \right), \quad (17)$$

where $\dot{M}_{d0} = 2\pi r_{\text{in}} \Sigma_{d0} = \text{const}$ is the disc accretion rate at the inner radius of the disc assuming the disc extends into $r_{\text{in}}(t = 0)$. As discussed in Sec. 3, we consider that the mean boundary layer velocity U is a factor $g \geq 1$ times larger than the local escape velocity, $U(r) = g(2GM/r)^{1/2}$. Additionally, we assume $H/r = (H/r)_i (r/r_i)^\beta$ with $\beta > 1/4$.

An estimate of the time t_{cr} at which $\hat{\Sigma}$ decreases to zero at $r_{\text{in}}(t = 0)$ follows from Equations (16) and (17) assuming $ut \gg r_{\text{in}}$,

$$t_{\text{cr}} \approx \frac{r_{\text{in}}(0)}{u} \left(\frac{\dot{M}_{d0} g \sqrt{2} v_{K_i}}{\dot{M}_w (H/r)_i v_w} \right)^{\frac{1}{\beta+1/2}}. \quad (18)$$

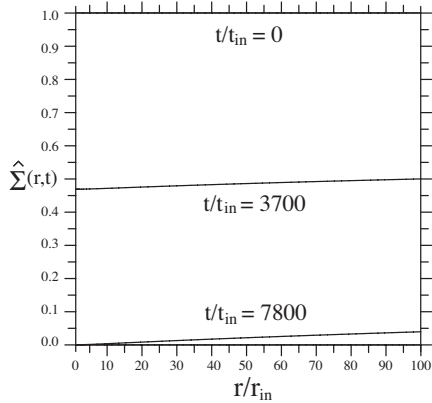


Figure 3: Evolution of the disc surface density $\hat{\Sigma}_d(r,t) = \Sigma_d(r,t)/\Sigma_d(r,0)$ for an illustrative case discussed in the text. The radius is measured in units of the initial inner radius of the disc, $r_{in}(t=0)$, which is taken to be $10r_\odot = 7 \times 10^{11}$ cm. Time is measured in units of $t_{in} = r_{in}/u = 257$ yr, where the accretion speed is $u = 86.3$ cm/s corresponding to a viscosity coefficient $\alpha = 10^{-2}$ and a disc half-thickness at r_{in} of $h_{in} = 0.025r_{in}$. Additionally, we have assumed $H/r = 0.03(r/r_{in})^\beta$ with $\beta = 0.3$ so that $(H/r)_{out} = 0.3$. Also, $U(r) = g(2GM/r)^{1/2}$ with $g = 2$ and $M = M_\odot$, which is twice the local escape speed.

Formally, t_{cr} is independent of r_{in} . The dominant factors determining this time-scale are u and $[v_w \dot{M}_w / (v_{Ki} \dot{M}_{d0})]$ with, for example, $t_{cr} \propto u^{-1} [v_{Ki} \dot{M}_{d0} / (v_w \dot{M}_w)]^{1.43}$ for $\beta = 0.3$.

Figure 3 shows the behavior of $\hat{\Sigma}(r,t)$ for an illustrative case where for $t > 0$, the stellar wind has $\dot{M}_w = 10^{-10} M_\odot/\text{yr}$ and $v_w = 10^3$ km/s, the initial disc accretion rate is $\dot{M}_{d0} = 10^{-8} M_\odot/\text{yr}$, and the viscosity coefficient is $\alpha = 0.01$. A central hole in the disc appears at $t/t_{in} \approx 7.8 \times 10^3$ when $\hat{\Sigma}(r_{in}, t) = 0$ at $t \approx 2 \times 10^6$ yr which is approximately equal to t_{cr} of Equation 18.

After a hole starts to form for $t > t_{cr}$, we can rewrite the normalizations to r_{in} in terms of normalizations to $r_{out} = \text{const.}$ For example, $H/r = (H/r)_{out} (r/r_{out})^\beta$. In this way we find for $t > t_{cr}$,

$$\frac{r_{\text{hole}}(t)}{r_{in}(0)} \approx 1 + 0.56 \left(\frac{t - t_{cr}}{t_{in}} \right)^{1.25}, \quad (19)$$

where $t_{in} = r_{in}(0)/u$. Evidently, the hole expands rapidly for $t > t_{cr}$.

5 Conclusions

This work develops an analytic model of the erosion of the gas component of discs caused by high-velocity magnetized stellar winds. The presence of the magnetic field leads to Reynolds numbers sufficiently large to cause

a strongly turbulent wind/disk boundary layer. This boundary layer entrains and carries away the disc gas. Strongly magnetized winds from young stars ($\lesssim 10^7$ yr) with discs are likely because the stars are known to rotate rapidly and to be strongly magnetized. We focus on the erosion of the gas component of the disc. Initially, the disc mass is constituted predominantly of gas, and furthermore the vertical scale-height of the gas is larger than that of the dust. However, further analysis is needed to understand the erosion of the dust.

Sample results for the evolution of the disc surface density $\hat{\Sigma}_d = \Sigma_d(r, t)/\Sigma(r, 0)$ are shown in Figure 3. The inner region of the disc surface density decreases more rapidly than that at larger radii with the result that a hole forms after a critical time t_{cr} . For the case shown, this time is about 2×10^6 yr. The critical time is proportional to the inverse accretion speed in the disc $u = \text{const}$ times the ratio \dot{M}_{d0}/\dot{M}_w raised to a power larger than unity, where \dot{M}_{d0} is the initial disc accretion rate and \dot{M}_w is the mass loss rate in the wind. More realistic models would have u dependent on space and time, and v_w and \dot{M}_w dependent on time as the star spins down.

Acknowledgments

We thank Prof. J. P. Lloyd for helpful discussions. This work was supported in part by NASA grants NNX11AF33G, NNX12AI85G, and NSF grant AST-1211318.

References

- Andrews S. M., Williams J. P., 2005, *ApJ*, 631, 1134
- Armitage, P.J., & Clarke, C.J. 1996, *MNRAS*, 280, 458
- Armitage P. J., 2010, *The Astrophysics of Planet Formation*. (Cambridge University Press: New York)
- Belcher J. W., & MacGregor K. B., 1976, *ApJ*, 210, 498
- Birnstiel, T., Pinilla, P., Andrews, S.M., Benisty, M., & Eercolano, B. 2013, *Instabilities and Structures in Proto-Planetary Disks*, eds. Barge, P., and Jorda, L., EPJ Web of Conferences 46
- Bouvier J., Cabrit S., Fernández M., Martín E. L., & Matthews J. M., 1993, *A&A*, 272, 176
- Braginskii S. I., 1965, *Review of Plasma Physics*, Vol. 1, (Consultants Bureau: New York)
- Clarke, C. J., Gendrin, A., & Sotomayor, M. 2001, *MNRAS*, 328, 485
- Espaillet, C., Calvet, N., D'Alessio, P., Bergin, E., Hartmann, L., Watson, D., Furlan, E., Najita, J., Forrest, W., McClure, M., Sargent, B., Bohac, C., & Harrold, S.T. 2007, *ApJ*, 664, L111

- Hartmann L., Calvet N., Gullbring E., & D'Alessio P., 1998, *ApJ*, 495, 385
- Hollenbach D. J., Yorke H. W., & Richstone D., 2000, in *Protostars and Planets IV*, eds. Mannings V., Boss A. P., & Russell S. S., (Univ. Arizona Press: Tuscon), p. 406
- Johns-Krull C. M., & Valenti J. A., 2000, in *Stellar Clusters and Associations: Convection, Rotation, and Dynamos*, eds. Pallavicini R., Micela G., & Sciortino S., Proceedings from ASP Conference, Vol. 198. Vol. 198, Measurements of stellar magnetic fields. San Francisco, CA, pp 371–380
- Johns-Krull C. M., 2007, *ApJ*, 664, 975
- Kuchner M.J. 2004, *ApJ*, 612, 1147
- Long M., Romanova M.M., & Lovelace R.V.E. 2005, *ApJ*, 634, 1214
- Lovelace R.V.E., Romanova M.M., & Bisnovatyi-Kogan G.S. 1999, *ApJ*, 514, 368
- Lovelace R. V. E., Romanova M. M., & Barnard A. W., 2008, *MNRAS*, 389, 1233
- Matt S., & Pudritz R. E., 2008a, *The Astrophysical Journal*, 678, 1109
- Matt S., & Pudritz R. E., 2008b, *ApJ*, 681, 391
- Michel F. C., 1969, *ApJ*, 158, 727
- Owen, J. E., Clarke, C. J., & Ercolano, B. 2012, *MNRAS*, 422, 1880
- Piétu, V., Dutrey, A., Guilloteau, S., Chapillon, E., & Pety, J. 2006, *A&A*, 430, L43
- Regály, Zs., Juhsz, A., Sndor, Zs., & Dullemond, C. P. 2012, *MNRAS*, 419, 1701
- Richling S., & Yorke H. W., 1997, *A&A*, 324, 317
- Romanova M. M., Ustyugova G. V., Koldoba A. V., & Lovelace R. V. E., 2005, *ApJ*, 635, L165
- Roy, C.J., & Blottner, F.G. 2006, *Prog. in Aerospace Sciences*, 42, 469
- Schlichting, H. 1968, *Boundary-Layer Theory*, (McGraw-Hill: New York), ch. 23
- Shakura N. I., & Sunyaev R. A., 1973, *A&A*, 24, 337
- Skrutskie M. F., Dutkevitch D., Strom S. E., Edwards S., & Strom K. M., 1990, *AJ*, 99, 1187
- Ustyugova G. V., Koldoba A. V., Romanova M. M., & Lovelace R. V. E., 2006, *ApJ*, 646, 304

Weber E. J., & Davis L., 1967, ApJ, 148, 217

Wolk S. J., & Walter F. M., 1996, AJ, 111, 2066

Zsom A., Ormel, C. W., Güttler C., Blum J., & Dullemond C. P., 2010,
A&A, 513, A57